Phase-controlled Fano resonance by the nanoscale optomechanics

Jian-Qi Zhang,[1] Yi Xu,[2] Keyu Xia,[3] Zhi-Ping Dai,[4] Wen Yang,[5,*] Shangqing Gong,[6,†] and Mang Feng[1,‡]

[1]*State Key Laboratory of Magnetic Resonance and Atomic and Molecular Physics, Wuhan Institute of Physics and Mathematics, Chinese Academy of Sciences - Wuhan National Laboratory for Optoelectronics, Wuhan 430071, China*

[2]*School of Physics and Electric Engineering, Guangzhou University, Guangzhou 510006, China*

[3]*ARC Centre for Engineered Quantum Systems, Department of Physics and Astronomy, Macquarie University, NSW 2109, Australia*

[4]*Department of Physics and Electronic Information Science, Hengyang Normal University, Hengyang 421008, China*

[5]*Beijing Computational Science Research Center, Beijing 100084, China*

[6]*Department of Physics, East China University of Science and Technology, Shanghai 200237, China*

(Dated: July 24, 2014)

Observation of the Fano line shapes is essential to understand properties of the Fano resonance in different physical systems. We explore a tunable Fano resonance by tuning the phase shift in a Mach-Zehnder interferometer (MZI) based on a single-mode nano-optomechanical cavity. The Fano resonance is resulted from the optomechanically induced transparency caused by a nano-mechanical resonator and can be tuned by applying an optomechanical MZI. By tuning the phase shift in one arm of the MZI, we can observe the periodically varying line shapes of the Fano resonance, which represents an elaborate manipulation of the Fano resonance in the nanoscale optomechanics.

PACS numbers: 42.50.Nn, 42.50.Wk, 42.25.Hz

arXiv:1407.5746v2 [physics.optics] 23 Jul 2014

Fano profiles are typically asymmetric line shapes, resulted from quantum interference between discrete energy states and a continuum spectrum [1]. Since the celebrated discovery by Fano [2], the Fano profiles have been observed in various physical systems with atoms [3–5], photons [6–9], and solid-state systems [10–12]. Recently, the Fano profile has also been studied based on the optomechanics [13], where a nano-mechanical resonator (NAMR) inside an optical cavity interacts with the cavity mode via the radiation pressure.

The field of the optomechanics has become a rapidly developing area of physics and nanotechnology over the past decades. Since the NAMR is very sensitive to the tiny external force, the study of the optomechanics is mainly motivated by the precision measurement, such as the ultra-sensitive detections of the mass [15], the charge number [16], the gravitational wave [17] and the displacement (or the force) [18, 19]. Moreover, there have been extensive interests in observing quantum properties of the NAMRs, including optomechanical entanglement [20–22], photon blockade [23, 24], carrier-envelope phase-dependent effect [25], and optomechanically induced transparency (OMIT) [26–28]. By adding more continuum spectra into the Fano resonance system, one can gain more degrees of freedom to manipulate the resonance interaction[32].

In this Letter, we focus on a tunable Fano profile generated by the quantum interference between a quasi-continuum light and an output light from the optomechanics, via the NAMR-induced OMIT. Such quantum interference is fulfilled by the MZI constructed by an optomechanical system and a phase shifter. The key point of our scheme is the phase tunable Fano profile, which is based on the unique characteristic of the OMIT. The output light from the optomechanics involves both symmetric and asymmetric components. Due to this reason, the Fano profile can be adjusted by tuning the phase in the second continuum light rather than by tuning the input light frequency[13, 14]. Moreover, our scheme presents an ideal case to control the Fano resonance of the optomechanical system by using a phase shifter outside the optomechanical system. Furthermore, compared with the conventional Fano profiles exhibiting sharp asymmetric Fano profiles in transmission or absorption [1], the Fano profile in our scheme can be tuned periodically, i.e., from a symmetric line shape [32] to an asymmetric one, and then back to a symmetric one. Inverted Fano profiles can be obtained by properly manipulating the phase shifter. We emphasize that, since there are some additional quantum interferences in optomechanics for the OMIT effect, our scheme based on the Mach-Zehnder interferometer (MZI) involves more interferences than in the conventional MZI, which might be practical for the precision measurement using NAMR-based optomechanics.

The core part in our scheme is an optomechanical system sketched in FIG.1, where a NAMR is suspended in an optical cavity composed of two fixed mirrors with identical finite transmission. The cavity mode, which is driven by a strong external field with the coupling strength ε_l and the frequency ω_l, interacts with the NAMR by a radiation pressure coupling. In addition, a weak probe light with the frequency ω_p is incident into the optical cavity, which is of a large bandwidth and can be considered as

*Corresponding author Email: yangw@csrc.ac.cn
†Corresponding author Email: sqgong@ecust.edu.cn
‡Corresponding author Email: mangfeng@wipm.ac.cn

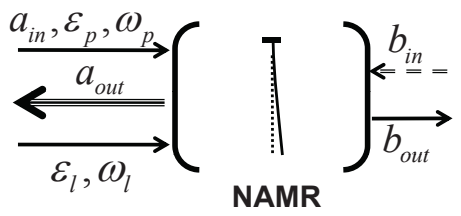

FIG. 1: Schematic diagram of an optomechanical system involving a NAMR. The cavity mirrors are highly reflected so that the cavity decay is small. b_{in} represents the input of a vacuum field, a_{out} and b_{out} indicate the reflected and transmitted lights from the optical cavity. Other denotations are defined in the text.

a quasi-continuum light with the OMIT effect. Then, in the rotating frame with the driving field frequency ω_l, the Hamiltonian for this system reads

$$\begin{aligned}\hat{H} &= -\hbar\Delta_c c^\dagger c + (\frac{p^2}{2m} + \frac{m\omega_m^2}{2}q^2) \\ &- \hbar g q c^\dagger c + (i\hbar\varepsilon_l c^\dagger + \text{ H.c. }),\end{aligned} \tag{1}$$

where $\Delta_c = \omega_c - \omega_l$ is the detuning of the driving field frequency ω_l from the bare cavity frequency ω_c, c is the bosonic annihilation operator of the cavity mode, p and q are the position and momentum operators of a NAMR with the mass m and the frequency ω_m, $g = \omega_c/L$ is the radiation pressure coupling between the cavity field and the NAMR with L being the cavity length [30].

A proper analysis of the system should involve the dissipations, such as the photon loss from the cavity and the Brownian noise from the environment. So the dynamics of the system is governed by the nonlinear quantum Langevin equations

$$\begin{aligned}\frac{\partial q}{\partial t} &= p/m, \\ \frac{\partial p}{\partial t} &= -m\omega_m^2 q + \hbar g c^\dagger c - \gamma_m p + \sqrt{2\gamma_m}\xi(t), \\ \frac{\partial c}{\partial t} &= -[2\kappa + i(\Delta_c - gq)]c + \varepsilon + \sqrt{2\kappa}(a_{in} + b_{in}),\end{aligned} \tag{2}$$

where γ_m and κ are introduced as the NAMR decay and the cavity decay, respectively. The quantum Brownian noise ξ comes from the coupling between the NAMR and the environment. The correlation of the noise operator is $\langle\xi(t)\xi(t')\rangle = N_{th}\delta(t-t')$ with $N_{th} = 1/(e^{\frac{\hbar\omega_m}{k_B T}} - 1)$ at a temperature $T > \hbar\omega_m/k_B$. Eq.(2) can be solved after all operators are linearized as the steady-state mean values plus the small fluctuations,

$$q = q_s + \delta q, \quad p = p_s + \delta p, \quad c = c_s + \delta c\,, \tag{3}$$

with δq, δp and δc being the small fluctuations around the corresponding steady-state values q_s, p_s and c_s, respectively.

After substituting Eq.(3) into Eq.(2), ignoring the second-order small terms, and introducing the Fourier transforms $f(t) = 1/2\pi\int_{-\infty}^{+\infty} f(\omega)e^{-i\omega t}d\omega$, we obtain the steady values $p_s = 0$, $q_s = \hbar g|c_s|^2/(m\omega_m^2)$, and $c_s = \varepsilon_l/(2\kappa + i\Delta)$ with $\Delta = \Delta_c - gq_s$. Then the solution of δc is identical to the one in Ref. [25],

$$\begin{aligned}\delta c(\omega) &= V(\omega)\xi(\omega) + E(\omega)[a_{in}(\omega) + b_{in}(\omega)] \\ &+ F(\omega)[a_{in}^\dagger(-\omega) + b_{in}^\dagger(-\omega)],\end{aligned} \tag{4}$$

with

$$\begin{aligned}V(\omega) &= igc_s[2\kappa - i(\Delta + \omega)]/d(\omega), \\ E(\omega) &= \sqrt{2\kappa}\{m[2\kappa - i(\Delta + \omega)](\omega^2 - \omega_m^2 + i\omega\gamma_m) \\ &- i\hbar g^2|c_s|^2\}/d(\omega), \\ F(\omega) &= -i2\sqrt{2\kappa}\hbar g^2 c_s^2/d(\omega), \\ d(\omega) &= m[\Delta^2 + (2\kappa - i\omega)^2](\omega^2 - \omega_m^2 + i\omega\gamma_m) \\ &+ 2\hbar g^2|c_s|^2\Delta.\end{aligned} \tag{5}$$

According to the input-output relation of the cavity [33], the output field from the port b_{out} is given by [27]

$$\begin{aligned}b_{out}(\omega) &= b_{in}(\omega) - \sqrt{2\kappa}\delta c(\omega) \\ &\simeq -\sqrt{2\kappa}E(\omega)a_{in}(\omega),\end{aligned} \tag{6}$$

where we have assumed that the input noises regarding b_{in}, $a_{in}^\dagger$ and ξ are negligible compared to the dominant contribution from the input channel a_{in} to the cavity [16, 26, 30].

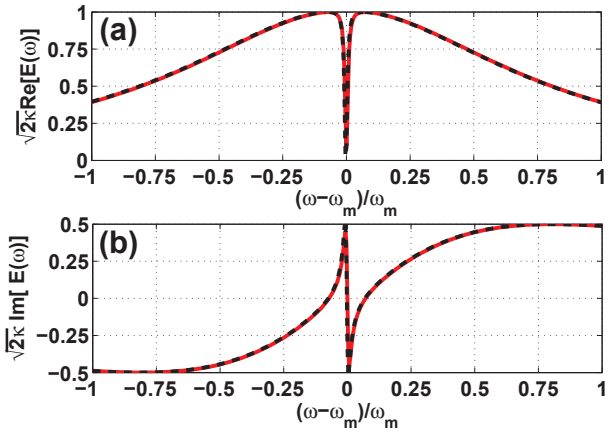

FIG. 2: (Color online) (a) The real component $\sqrt{2\kappa}Re[E(\omega)](= \sqrt{2\kappa}\Re[E(\omega)])$ of the transmission versus the normalized detuning $(\omega - \omega_m)/\omega_m$. (b) The imaginary component $\sqrt{2\kappa}Im[E(\omega)](= \sqrt{2\kappa}\Im[E(\omega)])$ of the transmission versus the normalized detuning $(\omega - \omega_m)/\omega_m$. The red solid lines (black dotted lines) represent the exact (approximate) solution using Eq.(5) [Eq.(7)]. We choose $\lambda_c \equiv 2\pi c/\omega_c = 400$ nm, $L = 1$ mm, $m = 1.45$ ng, $\kappa = 2\pi \times 10$ MHz, $\omega_m = 2\pi \times 30$ MHz, $\gamma_m = 2\pi \times 3$ kHz, $\Delta = 0.998\omega_m$ and $\varepsilon_l = \sqrt{2P\kappa/\hbar\omega_c}$ with $P = 5$ mW [26, 34, 35].

To further understand the transmission b_{out}, we employ the following conditions [26, 27]: (i) $\Delta \simeq \omega_m$ and (ii) $\omega_m \gg \kappa$. The first condition means that the optical cavity is driven by a red-detuned laser field which is on resonance with the optomechanical anti-Stokes sideband. The second condition is the well-known resolved sideband condition, which ensures a distinguishable splitting of the

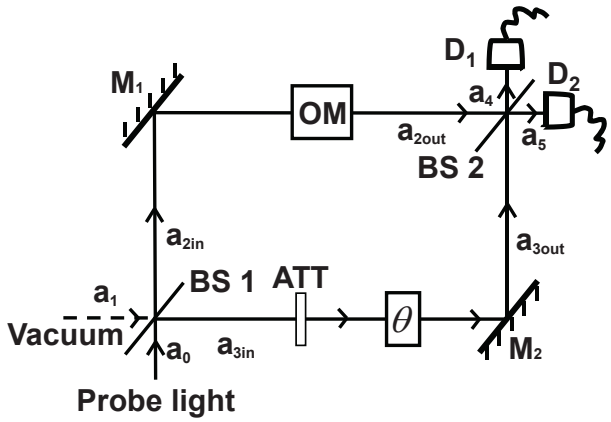

FIG. 3: Mach-Zehnder interferometer (MZI) involving an optomechanical cavity (OM). In the upper arm, the light is reflected by the mirror M_1 and then passes through the OM. The light in the lower arm first passes through an attenuator (ATT), and then experiences a phase shift θ. The two light beams interfere in the second beam splitter (BS2) at the output port before they are detected by the detectors D_1 and D_2.

normal mode [27]. Moreover, we assume $\omega \simeq \omega_m$ so that there is a strongest coupling between the NAMR and the cavity [26] with $\omega^2 - \omega_m^2 \simeq 2\omega_m(\omega - \omega_m)$. As a result, $E(\omega)$ in Eq.(5) can be reduced to

$$E(\omega) \simeq \frac{\sqrt{2\kappa}}{2\kappa - i(\omega - \omega_m) + \beta/[\gamma_m/2 - i(\omega - \omega_m)]}, \quad (7)$$

with $\beta = \dfrac{\hbar g^2 |c_s|^2}{2m\omega_m}$.

When the driving field and the quasi-continuum probe light are simultaneously incident into the optomechanical cavity, only the probe light with the frequency at $\omega_p = \omega_c + \omega_m$ can be reflected from the output port a_{out}, and the rest transmits to the port b_{out}. The corresponding transmission $\sqrt{2\kappa}E(\omega) = -b_{out}(\omega)/a_{in}(\omega)$ involves a symmetric real part (with the even symmetry) and an asymmetric imaginary part (with the odd symmetry) (see FIG.2). The good agreement between the results by FIG.5 and Eq.(7) indicates that the transmitted light is resulted from the OMIT effect [26, 27]. This output light from the optomechanics can be treated as a quasi-continuum light excluding a single-mode component at the frequency $\omega_l - \omega_m$. To the best of our knowledge, this kind of output light for the phase-tuning Fano profile is an unique characteristic of our model involving the optomechanics and has never been reported previously in other physical systems.

We present below how to control the Fano profile via phase-tuning in one of the arms of the MZI. The setup for such tunable Fano profiles is presented in FIG.3, where the probe light is a quasi-continuum field. After this probe light $a_0(\omega)$ along with the vacuum field $a_1(\omega)$ is sent into the first beam splitter (BS1) of the MZI, the two fields are split into two superposition fields as [36],

$$\begin{aligned} a_{2in}(\omega) &= [a_0(\omega) + ia_1(\omega)]/\sqrt{2}, \\ a_{3in}(\omega) &= [a_1(\omega) + ia_0(\omega)]/\sqrt{2}\,. \end{aligned} \quad (8)$$

We assume that the optical-path difference between the two arms of the MZI is integral times of the wavelength. When the light beam in $a_{2in}(\omega)$ [$=a_{in}(\omega)$ in FIG.1] passes through the optomechanical system, the output light from the optomechanics owns both symmetric real and asymmetric imaginary components. On the other hand, the quasi-continuum light in the lower arm $a_{3in}(\omega)$ passes through an attenuator (ATT) and experiences a phase shift θ. Thus the modes $a_{2in}(\omega)$ and $a_{3in}(\omega)$ can be written as

$$\begin{aligned} a_{2out}(\omega) &= -\sqrt{2\kappa}\mu E(\omega)[a_0(\omega) + ia_1(\omega)]/\sqrt{2}, \\ a_{3out}(\omega) &= e^{i\theta}[a_1(\omega) + ia_0(\omega)]/\sqrt{2}, \end{aligned} \quad (9)$$

where $\mu^2 = |a_{2out}(\omega)/a_{3out}(\omega)|^2$ depends on the amplitude transmission of the optomechanics as well as the ATT absorption in the MZI. The output light $a_{2out}(\omega)$ is much weakened due to the highly reflected mirror of the optomechanical cavity, and excludes a single-mode component at the frequency $\omega_l - \omega_m$. The other light $a_{3out}(\omega)$ is a quasi-continuum light, which is also weak after experiencing the ATT. If we assume the light $a_{2out}(\omega)$ to be of the unit intensity, the phase-shifted light $a_{3out}(\omega)$ is of the intensity $1/\mu^2$. The two lights interfere in the second beam splitter (BS2) before they are measured by the detectors. The corresponding output lights are given by

$$\begin{aligned} a_4(\omega) &= -\sqrt{2\kappa}\mu E(\omega)[a_0(\omega) + ia_1(\omega)]/2 \\ &\quad - e^{i\theta}[a_0(\omega) - ia_1(\omega)]/2\,, \\ a_5(\omega) &= -\sqrt{2\kappa}\mu E(\omega)[ia_0(\omega) + a_1(\omega)]/2 \\ &\quad + e^{i\theta}[a_1(\omega) + ia_0(\omega)]/2\,. \end{aligned} \quad (10)$$

As an example, we consider below the output spectrum of the mode $a_4(\omega)$, defined by

$$\left\langle a_4^\dagger(-\Omega)a_4(\omega)\right\rangle = 2\pi S_{out}(\omega)\delta(\Omega + \omega), \quad (11)$$

where S_{out} is the spectrum of the output light, which will be defined later.

To observe this output spectrum, we introduce the correlation functions of the quasi-continuum probe field and the input vacuum field, respectively, [37]

$$\left\langle a_0^\dagger(-\Omega)a_0(\omega)\right\rangle = 2\pi S_{in}(\omega)\delta(\omega + \Omega), \quad (12)$$

and

$$\left\langle a_1(-\Omega)a_1^\dagger(\omega)\right\rangle = 2\pi\delta(\omega + \Omega). \quad (13)$$

with $S_{in}(\omega)$ being the spectrum of the input field. Substituting Eq.(12) and Eq.(13) into Eq.(11), the spectrum of the output field $a_4(\omega)$ is given by

$$S_{out}(\omega) = R(\omega)S_{in}(\omega), \quad (14)$$

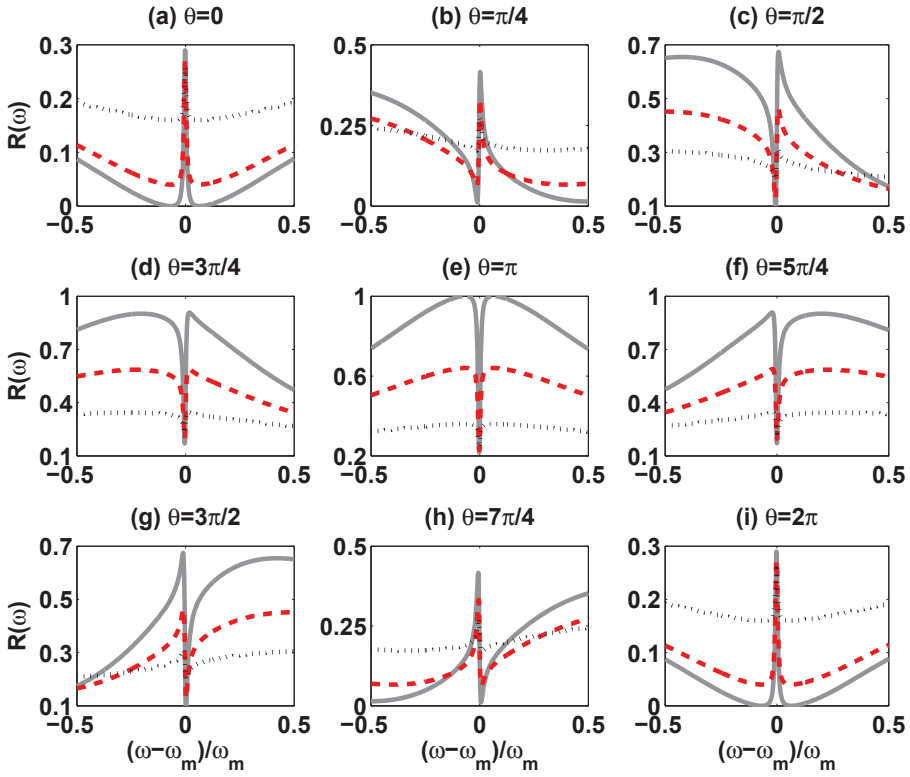

FIG. 4: (Color online) The profiles of the Fano resonance in variation with θ and μ, where the parameters take the same values as in FIG.2. The curves in each panel: the gray solid, the red dashed and the black dot correspond to μ =1.0, 0.6 and 0.2, respectively.

with

$$R(\omega) = R_c(\omega) + \mu^2 R_s(\omega) + \mu R_{cs}(\omega)\,, \quad (15)$$

$$R_c(\omega) = 1/4\,, \quad (16)$$

$$R_s(\omega) = \kappa|E(\omega)|^2/2\,, \quad (17)$$

$$R_{cs}(\omega) = \frac{\sqrt{\kappa}}{2}(\Re[E(\omega)]\cos\theta + \Im[E(\omega)]\sin\theta) \quad (18)$$

where $R_s(\omega)$ indicates the quantum interference in the output light from the optomechanics (self-interference), while $R_{cs}(\omega)$ attributes to the compound interference (cross-interference) between the quasi-continuum light in the lower arm and the output light from the optomechanics in the upper arm. Different from the conventional MZI, the optomechanical output light itself is the result of the interference caused by the OMIT, which yields $R_{cs}(\omega)$ containing a symmetric component $\Re[E(\omega)]$ and an asymmetric one $\Im[E(\omega)]$. What is more, the contributions regarding the symmetric and asymmetric parts can be adjusted by the phase shift at our will. As a result, the Fano profiles in our scheme are fully controllable by the phase tuning, whose effect can be observed directly from the output spectrum of the MZI. As demonstrated in FIG.4, the Fano profiles change periodically in an axially symmetric fashion, where the panels (a-d) are, respectively, inverted to the panels (e-h).

To further understand FIG.4, we plot in FIG.5 the curves of $\kappa|E(\omega)|^2$ and $\sqrt{\kappa/2}\Re[E(\omega)]$, which are in good agreement with each other. This implies $\kappa|E(\omega)|^2 \simeq \sqrt{\kappa/2}\Re[E(\omega)]$. In fact, we may also understand FIG.4 from following analysis. In the case of $\cos\theta = -1$, $R(\omega)$

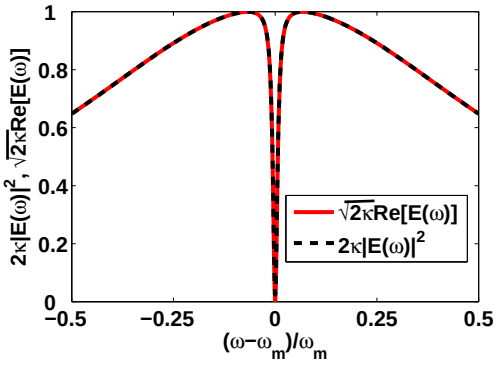

FIG. 5: (Color online) The comparison between the real part ($\sqrt{2\kappa}Re[E(\omega)] = \Re[\sqrt{2\kappa}E(\omega)]$) and the square term ($2\kappa|E(\omega)|^2$) of the output light from the optomechanical cavity. The good agreement implies $\sqrt{2\kappa}Re[E(\omega)] \simeq 2\kappa|E(\omega)|^2$.

in Eq.(15) can be reduced to

$$\begin{aligned} R(\omega) &= 1/4 + \mu^2\kappa|E(\omega)|^2/2 - \mu\sqrt{\kappa/2}\Re[E(\omega)] \\ &\simeq 1/4 + (\mu^2 - 2\mu)\sqrt{\kappa/2}\Re[E(\omega)]/2, \end{aligned} \quad (19)$$

with $\mu^2 - 2\mu < 0$ for $0 < \mu \leq 1$. It indicates that the profile of $R(\omega)$ is very similar to that of the function $-\sqrt{2\kappa}\Re[E(\omega)]$ which is inverted with respect to the function $\sqrt{2\kappa}\Re[E(\omega)]$.

In conclusion, motivated by recent development of nanotechnology, we have studied the tunable Fano profile in an optomechanical system by the phase tuning in the

MZI. These phase-controlled Fano profiles are generated by two kinds of quantum interferences and vary periodically under our exact control. Since the NAMR has become a state-of-the-art device for metrology and the Fano profile in our scheme involves more interferences, we believe that our elaborate manipulation of the Fano resonance would arouse widespread application, such as the precision measurement, with the NAMR-based optomechanics.

We would like to thank Profs. Jin-Hui Wu and Kai-Jun Jiang, and Dr. Yi Zhang for helpful discussion. The work is supported by the National Fundamental Research Program of China (Grant Nos. 2012CB922102, 2012CB922104, and 2009CB929604), the National Natural Science Foundation of China (Grant Nos. 10974225, 60978009,11174027, 11174370, 11274036, 11304366, 11274112, 11204080, 11322542 and 61205108), and the China Postdoctoral Science Foundation (Grant Nos. 2013M531771 and 2014T70760).

[1] A. E. Miroshnichenko, S. Flach, and Y. S. Kivshar, Rev. Mod. Phys. **2010**, 82, 2257.
[2] U. Fano, Nuovo Cimento **1935**, 12, 154–161.
[3] U. Fano, Phys. Rev. **1961**, 124, 1866–1878.
[4] T. Kraemer, M. Mark, P. Waldburger, J. G. Danzl, C. Chin, B. Engeser, A. D. Lange, K. Pilch, A. Jaakkola, H.-C. Nagerl, and R. Grimm, Nature (London) **2006**, 440, 315–318.
[5] P. M. Anisimov, J. P. Dowling, and B. C. Sanders Phys. Rev. Lett. **2011**, 107, 163604.
[6] A. E. Miroshnichenko, S. F. Mingaleev, S. Flach, and Y. S. Kivshar, Phys. Rev. E **2005**, 71, 036626.
[7] S. F. Mingaleev, A. E. Miroshnichenko, Y. S. Kivshar, and K. Busch, Phys. Rev. E **2006**, 74, 046603.
[8] N. Verellen, Y. Sonnefraud, H. Sobhani, F. Hao, V. V. Moshchalkov, P. V. Dorpe, P. Nordlander, and S. A. Maier, Nano Lett. **2009**, 9, 1663–1667.
[9] A. E. Miroshnichenko, Y. Kivshar, C. Etrich, T. Pertsch, R. Iliew, and F. Lederer, Phys. Rev. A **2009**, 79, 013809.
[10] S. Flach, A. E. Miroshnichenko, V. Fleurov, and M. V. Fistul, Phys. Rev. Lett. **2003**, 90, 084101.
[11] Y. S. Joe, A. M. Satanin, and C. S. Kim, Phys. Scr. **2006**, 74 259–266.
[12] R. Hanson, L. P. Kouwenhoven, J. R. Petta, S. Tarucha, and L. M. K. Vandersypen, Rev. Mod. Phys. **2007**, 79 1217–1265.
[13] K. Qu, and G. S. Agarwal, Phys. Rev. A **2013**, 87, 063813.
[14] Q. Zhang, J. J. Xiao, X. M. Zhang, Y. Yao, and H. Liu, Opt. Exp. **2013** 21 6601-6608.
[15] K. L. Ekinci, Y. T. Yang, and M. L. Roukes, J. Appl. Phys. **2004**, 95, 2682.
[16] J. -Q. Zhang, Y. Li, M. Feng, and Y. Xu, Phys. Rev. A **2012**, 86, 053806.
[17] B. Abbott *et al.* Phys. Rev. Lett. **2005** , 95, 221101.
[18] F. Marquardt, and S. M. Girvin, Physics **2009**, 2, 40.
[19] S. Forstner, S. Prams, J. Knittel, E. D. van Ooijen, J. D. Swaim1, G. I. Harris, A. Szorkovszky, W. P. Bowen, and H. Rubinsztein-Dunlop, Phys. Rev. Lett. **2012**, 108, 120801.
[20] S. Mancini, V. Giovannetti, D. Vitali, and P. Tombesi, Phys. Rev. Lett. **2002**, 88, 120401.
[21] D. Vitali, S. Gigan, A. Ferreira, H. R. Bohm, P. Tombesi, A. Guerreiro, V. Vedral, A. Zeilinger, and M. Aspelmeyer, Phys. Rev. Lett. **2007**, 98, 030405.
[22] M. J. Hartmann and M. B. Plenio, Phys. Rev. Lett. **2008**, 101, 200503.
[23] P. Rabl, Phys. Rev. Lett. **2011**, 107, 063601.
[24] A. Nunnenkamp, K. Borkje, and S. M. Girvin, Phys. Rev. Lett. **2011**, 107, 063602.
[25] H. Xiong, L.-G. Si, X.-Y. Lv, X. Yang and Y. Wu, Opt. Lett. **2013**, 38, 353-355.
[26] G. S. Agarwal, and S. Huang, Phys. Rev. A **2010**, 81, 041803.
[27] S. Weis, R. Riviere, S. Deleglise, E. Gavartin, O. Arcizet, A. Schliesser, and T. J. Kippenberg, Science **2010**, 330, 1520.
[28] H. Xiong, L.-G. Si, A.-S. Zheng, X. Yang and Y. Wu, Phys. Rev. A **2012**, 86, 013815.
[29] A. H. Safavi-Naeini, T. P. M. Alegre, J. Chan, M. Eichenfield, M. Winger, Q. Lin, J. T. Hill, D. Chang, and O. Painter, Nature (London) **2011**, 472, 69–73.
[30] G. S. Agarwal and S. Huang, Phys. Rev. A **2012**, 85, 021801.
[31] J. P. Connerade, *Highly Excited Atoms*; Cambridge University Press: Cambridge, 1998.
[32] Y. Xu, and A. E. Miroshnichenko, Phys. Rev. A **2011**, 84, 033828.
[33] D. F. Walls and G. J. Milburn, Quantum Optics; Springer-Verlag: Berlin, 1994.
[34] S. Groblacher, K. Hammerer, M. Vanner, and M. Aspelmeyer, Nature (London) **2009**, 460, 724.
[35] J. D. Thompson, B. M. Zwickl, A. M. Jayich, F. Marquardt, S. M. Girvin, and J. G. E. Harris, Nature (London) **2008**, 452, 72.
[36] C. C. Gerry, and P. Knight, Introductory Quantum Optics; Cambridge University Press: New York, 2005
[37] S. Huang, and G. S. Agarwal, Phys. Rev. A **2009**, 79, 013821.
[38] Ph. Durand, I. Paidarova, and F. X. Gadea, J. Phys. B: At. Mol. Opt. Phys. **2001**, 34, 1953.